IRON-BASED NANOPARTICLES AND THEIR EFFECTS ON PLANTS: OUTLOOK AND FIRST RESULTS

Zoltán Klencsár, Gyula Tolnai, Zoltán Sándor, Zoltán May, Ervin Gy. Szabó, Péter Németh, László Szabó

Institute of Materials and Environmental Chemistry, Research Centre for Natural Sciences, Hungarian Academy of Sciences, Magyar tudósok körútja 2, 1117 Budapest, Hungary

Krisztina Kovács, Ernő Kuzmann, Zoltán Homonnay

Institute of Chemistry, Eötvös Loránd University, Pázmány P. s. 1/A, 1117 Budapest, Hungary

Fruzsina Pankaczi, Zita Fülöp, Zsuzsanna Farkas, Edit Ludmerszki, Ádám Solti, Ferenc Fodor

Institute of Biology, Eötvös Loránd University, Pázmány P. s. 1/A, 1117 Budapest, Hungary

1. Introduction

On account of their diverse and peculiar physicochemical properties, the magnitude and importance of production and industrial utilization of **manufactured nanoparticles (MNPs)** has been increasing rapidly in recent years [1]. According to global estimates [2], the total worldwide production of nanomaterials exceeded the order of 10^5 t/year already in 2012. It is inevitable that a considerable fraction of the produced nanoparticles will finally find its way from the industry and consumer products to different environmental compartments such as air, water and soil [3]. Despite growing concerns regarding the **environmental risks of MNPs**, as of today, knowledge about their transport, possible transformations, final fate and concentration in the ecosystems is scarce [3]. Even more alarming is the lack of comprehensive knowledge and understanding of the nature and mechanisms of the effects of MNPs on their possible host ecosystems and the associated living organisms such as algae, plants, and fungi, which are expected to be affected by an exposure to MNPs [4].

Plants may be exposed to MNPs in the atmosphere (through leaves) as well as in the soil (via roots). Airborne MNPs may directly enter plants through stomata and bases of trichomes, as well as they may lead to the obstruction of stomata with associated alteration of the leaves' gas exchange and thus photosynthesis. A direct physical interaction between the roots and MNPs polluting the soil may take place via endocytosis during the growth of root hair cells. **Nanoparticles with a diameter less than about 20 nm may also pass through the plant cell wall and reach the plasma membrane of plant cells.** Direct chemical interaction can take place between nanoparticles and root secretions in the rhizosphere, where—prior to potential uptake by the plant—metals can participate in chemical reactions leading to their solubilization via reduction and/or chelation.

Suitable **MNPs** may also serve **as nutrient reservoirs** in their host ecosystem. For high quality and efficient crop production, it is inevitable to ensure optimal nutrition for the plants: in case of low-quality soil (such as those with high soil pH), missing nutrients should be supplied by appropriate fertilizers. Insufficient supply of iron, for example, hampers chlorophyll biosynthesis, leading to slow growth, low plant biomass and nutrition value (Figure 1). Controlled exposure to selected iron-containing nanoparticles **may** therefore also turn out to **be beneficial to ecosystems** involving plants.

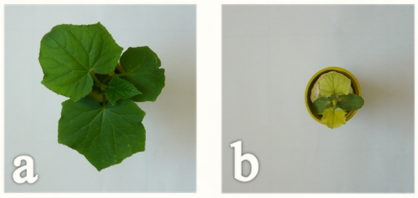

Figure 1. Illustration of the effect of insufficient iron supply on the development of cucumber plant: a, plant grown under normal conditions, b, plant grown under conditions with insufficient iron supply.

2. Aim of the work

In the frame of the present study we have prepared iron(III) oxide-hydroxide and iron-cobalt alloy nanoparticles with the aim to explore their effects on cucumber (Cucumis sativus) plants via controlled plant-growth experiments.

3. Experimental

Fe-Co alloy nanoparticles were prepared via wet chemical synthesis, by using iron(III) chloride hexahydrate and cobalt(II) acetate as precursors with aluminium powder and ammonium fluoride applied as reducing materials as described in [5]. Stable **colloid suspension of iron(III)-oxihydroxide nanoparticles** (**FH1**) was prepared via wet chemical synthesis with a concentration of ~ 0.37 mg/cm^3 for the colloidal fractions. The corresponding iron concentration was estimated to be ~ 0.26 mg/cm^3 [6]. For the XRD measurement a **powder sample** (**FH2**) was prepared from an analogous colloid suspension.

A wide range of experimental techniques—XRD, TEM, SEM, EDX, ICP-MS/OES, EPR/FMR and ^{57}Fe Mössbauer spectroscopy (^{57}Fe MS)—was applied in order to assess the attributes of the prepared nanoparticles and those of the plant samples. The experiments were carried out by the following equipments. Philips PW3710 based PW1050 Bragg-Brentano goniometer system used with Cu Kα radiation along with graphite monochromator (XRD), Morgagni 268D (100 kV) transmission electron microscope (TEM), Zeiss EVO40 XVP scanning electron microscope equipped with an Oxford INCA EDX spectrometer (SEM, EDX), Thermo Scientific "iCAP Qc" (ICP-MS) and Spectro Genesis (ICP-OES) spectrometers, Bruker ElexSys E500 X-band spectrometer (EPR/FMR), WISSEL spectrometer applied in transmission geometry along with a source of ^{57}Co in Rh matrix providing the γ-rays with ca. 20 mCi activity (^{57}Fe MS).

The **composition of Fe-Co alloy nanoparticles** was checked via ICP-MS and ^{57}Fe MS measurements on two separate (nearly equiatomic) alloy samples with slightly different Fe concentrations as well as via EDX carried out on their oxidized counterparts, where the three methods were found to reflect the different iron concentrations of the two samples with remarkable consistency [5]. A further batch of Fe-Co alloy nanoparticles was then prepared for the plant-growth experiments, in which case ^{57}Fe MS was used to ascertain the iron concentration of the alloy.

Plant growth experiments were carried out in hydroponics. In the case of Fe-Co alloy nanoparticles the experiments aimed at the exploration of **potentially toxic effects** that may be expected on account of the known phytotoxic nature of Co [7]. Accordingly, the alloy was administered to healthy plants in high concentrations (including either 0.1 mM or 1 mM of Fe) for a 12-days period. In contrast, the FH1 ferric-oxide-hydroxide colloid suspension was administered to iron deficient plants in lower concentrations (including 0.01 mM of iron) for a 1-week period in order to explore whether the plant can make use of the nanoparticles in a way that leads to its **regeneration**. After the nanoparticle treatments the health status of the plants was quantified by measuring the chlorophyll concentration in their leaves.

4. Characterization of nanoparticles

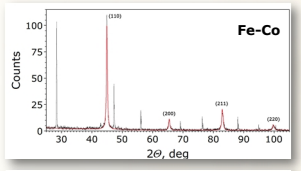

Figure 2. Cu Kα powder **X-ray diffractogram** of the **Fe-Co alloy** nanoparticles used in the plant growth experiments. Reflections belonging to the bcc alloy phase are marked with corresponding Miller indices and the outline of the fitting curve. Most narrow peaks belong to Si powder deliberately added to the sample for calibration purposes. The small peak at $2\theta \approx 43$ deg may belong to the minor ferric-oxide-hydroxide phase that shows up as a small doublet in the corresponding ^{57}Fe Mössbauer spectrum (Figure 3). Analysis of the diffractogram leads to a cubic lattice parameter of $a \approx 0.2850$ nm and a mean crystallite size of $d \approx 36$ nm, in good agreement with our previous results [5], which confirms the successful preparation of the Fe-Co alloy nanoparticles.

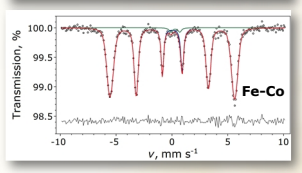

Figure 3. Room-temperature **^{57}Fe Mössbauer spectrum** of the **Fe-Co alloy** nanoparticles used in the plant growth experiments. The spectrum clearly reflects the presence of Fe-Co alloy in the form of a major sextet component displaying pronounced line broadening due to the presence of a large variety of iron atomic environments. The latter evidences a random distribution of Fe and Co atoms over the α and β sites of the bcc lattice. A small doublet component refers to the presence of a ferric-oxide-hydroxide minority phase that is a side product of the preparation procedure [5]. A fit of the sextet component to a model assuming binomial probability distribution of the number of iron atoms as nearest and next-nearest neighbor to a selected iron atom leads to an iron concentration of 56(3)%, confirming a nearly equiatomic alloy composition of ca. $Fe_{0.56}Co_{0.44}$.

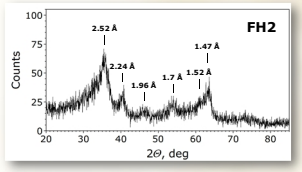

Figure 4. Cu Kα powder **X-ray diffractogram** of the **FH2** ferric-oxide-hydroxide sample. The indicated six broad reflections are a clear fingerprint of 6-line ferrihydrite, a poorly crystalline ferric-oxide-hydroxide [6,8]. The interplanar distances indicated for the associated peaks are in good agreement with corresponding literature data [8]. The width of the reflections is consistent with a crystallite size of 4-5 nm. There is a shoulder of the most intense peak at $2\theta \approx 33$ deg that may refer to the presence of extremely small (~ 1-2 nm) hematite nanoparticles in the sample [8].

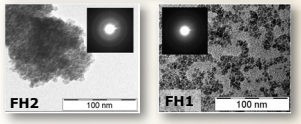

Figure 5. Transmission electron microscopy images of the **FH2** and **FH1** ferric-oxide-hydroxide samples, with the corresponding electron diffraction patterns shown as insets. The characteristic particle size is ~ 5 nm in both cases, in good agreement with the crystallite size observed for FH2 (Figure 4). The structure of characteristic interplanar distances reflected by the electron diffraction patterns corresponds well to that of the XRD reflections of FH2 (Figure 4), and thereby indicates that particles in the FH1 colloid suspension have a structure similar to that of particles in the powder FH2.

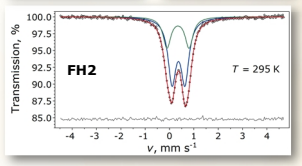

Figure 6. Room-temperature **^{57}Fe Mössbauer spectrum** of the FH2 ferric-oxide-hydroxide sample. The spectrum can be decomposed into two Lorentzian doublets with parameters ($\delta_1 \approx 0.37$ mm/s, $\Delta_1 \approx 0.53$ mm/s, $\delta_2 \approx 0.35$ mm/s, $\Delta_2 \approx 0.9$ mm/s) and a spectral area ratio (~2:1) close to the corresponding parameters of β-FeOOH (akaganéite) [9], which confirms that iron atoms in the FH2 nanoparticles have atomic environments corresponding to those expected to occur in ferric-oxide-hydroxide.

5. Plant growth experiments

In **toxicity experiments** 12-days administration of 0.1 mM iron-equivalent **Fe-Co alloy nanoparticles** to healthy plants **led to a pathological plant state** with symptoms akin to those of iron deficiency chlorosis: strongly hindered growth leading to low biomass and low chlorophyll levels leading to yellowish leaves. Tenfold increase in the Fe-Co concentration further amplified the deterioration of the plant that could hardly develop in comparison with a corresponding control.

With respect to healthy control plants, the administration of Fe-Co resulted in extreme high cobalt concentration and simultaneously decreased Fe concentration levels in the plants (Figure 7), indicating that the observed pathological plant state developed due to **cobalt poisoning**. This result appears to refer to an interaction taking place between the plant and the applied nanoparticles.

With respect to the control (with ~ 2 mg Chl / g fw), in the Fe-Co treated plants chlorophyll concentration levels were found to be reduced by roughly an order of magnitude, the reduction being more pronounced when the higher (1 mM) concentration of Fe-Co was applied.

In **regeneration experiments** the FH1 colloid suspension sample was found to be an efficient iron source for iron deficient cucumber plants (Figure 8). Plants grown under Fe-deficient conditions for 2 weeks recovered as a result of 1 week 0.01 mM FH1 administration by reaching iron concentration levels equal to or higher than that of the healthy control.

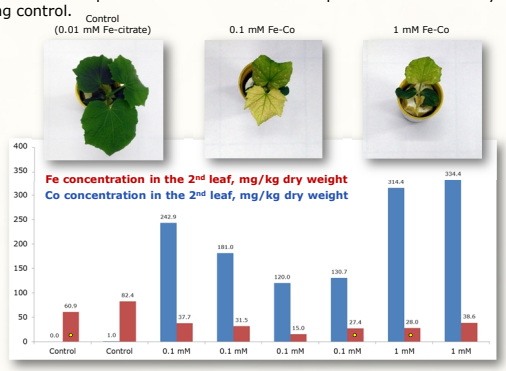

Figure 7. Effect of 12-days long Fe-Co alloy administration on the development of cucumber plants (previously grown on 0.01 mM Fe-citrate for 9 days) in comparison with healthy control grown continuously on 0.01 mM Fe-citrate. Typical results are illustrated as photos on the top, whereas the 2nd leaf's resulting Fe and Co concentration levels determined via **ICP-OES** measurements in individual cases are shown as bars for different Fe-Co concentrations underneath. Yellow dots denote cases for which EPR spectra are given in Figure 9 (top row).

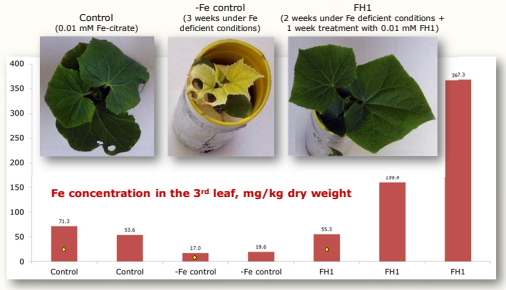

Figure 8. Effect of 1-week long FH1 colloid suspension sample administration on the development of cucumber plants (previously grown under Fe-deficient conditions for 2 weeks) in comparison with healthy control grown continuously on 0.01 mM Fe-citrate, and -Fe control that was continuously grown under Fe-deficient conditions. Typical results are illustrated as photos on the top, whereas the 3rd leaf's resulting Fe concentration levels determined via **ICP-OES** measurements in individual cases are shown as bars underneath. Yellow dots denote cases for which EPR spectra are given in Figure 9 (bottom row).

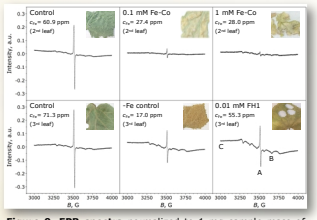

Figure 9. EPR spectra normalized to 1 mg sample mass of selected dried leaves of cucumber plant samples corresponding to the cases marked with a yellow dot on Figures 7 and 8. The three EPR signals generally observed in dried leaf samples are marked with A, B and C. Photos of dried leaf sample parts illustrate the apparent health status of the source plants.

X-band EPR spectroscopy measurements (Figure 9) performed on dried leaves of the plants in general revealed three distinct signals with $g \approx 2$: a narrow ($\Gamma_{pp} \approx 7$ G) isotropic singlet (**A**) at $g \approx 2.002(1)$ that may originate from free radicals (presumably of the semiquinone type formed via the oxidation of polyphenolic plant compounds) usually found in organic plant products, a broadened sextet component (**B**) related to presumably protein-bound, high-spin Mn^{2+} species, and a very broad (Γ_{pp} in the order of 500 G) underlying peak (**C**) associated with exchange-coupled transition metals, presumably mainly iron. We have found that the specific intensity of peak **A** correlates with the chlorophyll concentration of leaves with a linear correlation coefficient of $r \approx +0.9$, leaves of healthier plants tending to exhibit an **A** signal with larger specific intensity.

6. Conclusions

Our results underline the possibility of interactions between plants and nanoparticles by revealing that iron(III) oxide-hydroxide and Fe-Co alloy nanoparticles are both able to influence the quality and productivity of cucumber plants grown in hydroponics, the effects being essentially favorable when iron(III) oxide-hydroxide and essentially toxic when Fe-Co alloy nanoparticles are administered to the plant.

Acknowledgement. Financial support from the National Research, Development and Innovation Office - NKFIH/OTKA (K115913 and K115784) is gratefully acknowledged.

References

[1] A. Bour, F. Mouchet, J. Silvestre, L. Gauthier, E. Pinelli: *J. Hazardous Materials* **283** (2015) 764.
[2] F. Piccinno, F. Gottschalk, S. Seeger, B. Nowack: *J. Nanopart. Res.* **14** (2012) 1109.
[3] J.D. Posner: *Nano Today* **4** (2009) 114.
[4] E. Navarro, A. Baun, R. Behra, N.B. Hartmann, J. Filser, A. Miao, A. Quigg, P.H. Santschi, L. Sigg: *Ecotoxicology* **17** (2008) 372.
[5] Z. Klencsár, P. Németh, Z. Sándor, T. Horváth, I.E. Sajó, S. Mészáros, J. Mantilla, J.A.H. Coaquira, V.K. Garg, E. Kuzmann, Gy. Tolnai: *J. Alloys and Compounds* **674** (2016) 153.
[6] Z. Homonnay, Gy. Tolnai, F. Fodor, Á. Solti, K. Kovács, E. Kuzmann, A. Ábrahám, E.Gy. Szabó, P. Németh, L. Szabó, Z.Klencsár: *Hyperfine Interactions* **237** (2016) 127.
[7] W.B. Healy, S. Cheng, W.D. McElroy: *Archives of Biochemistry and Biophysics* **54** (1955) 206.
[8] D. Carta, M.F. Casula, A. Corrias, A. Falqui, G. Navarra, G. Pinna: *Mat. Chem. Phys.* **113** (2009) 349.
[9] E. Murad: *Clay Minerals* **14** (1979) 273–283.